Photonics applied to Coherent Radar Networks for Border Security

S. Maresca*[a], G. Serafino[b], F. Scotti[b], L. Lembo[ac], P. Ghelfi[b] and A. Bogoni[ab]

[a]TeCIP Institute, Scuola Superiore Sant'Anna, Pisa, Italy;
[b]PNTLab, Consorzio Nazionale Interuniversitario per le Telecomunicazioni (CNIT), Pisa, Italy;
[c]Vallauri Institute, Centro di Supporto e Sperimentazione Navale (CSSN), Livorno, Italy.

ABSTRACT

This paper investigates the target detection and localization capabilities of a centralized radar network with widely separated antennas in the framework of maritime border security. The proposed system takes advantage from photonic technology for signal generation/detection and signal distribution between the central and the remote radar nodes. Such a solution allows to achieve the necessary level of time and phase synchronization to benefit from the coherent multiple input multiple output (MIMO) paradigm for very high cross-range resolution.

The proposed photonics-based radar network is developed within the NATO-funded "Multistatic and multi-band coherent radar fleet for border security (SOLE)" project. Currently, the radar network architecture consists of two transmit/receive radar front-ends, for a total of four coherent virtual channels, employing linear frequency modulated pulses in time diversity at 9.7 GHz with 100 MHz bandwidth. The system has been operated in a preliminary down-scaled outdoor scenario for detecting two collaborative closely-spaced moving targets. With respect to the nominal aperture of the antenna, the cross-range resolution has been improved by a factor of five. The preliminary results demonstrate the impact of photonics applied to coherent centralized MIMO radars and suggest the possibility to soon endow the radar network with high-performance radar imaging capabilities.

Keywords: Maritime border security, centralized radar network, MIMO radar, coherence, widely-distributed antennas, photonics-based radar, radio-over-fiber system.

1. INTRODUCTION

Motivated by the ever-evolving operative conditions and number/variety of possible threats, radar-based border surveillance applications, especially in the maritime domain, see a predominance of solutions based on sensor fusion. Standalone monostatic/bistatic radars cannot meet all the required mission tasks. They are subject to strong target fluctuations, i.e. the spatial/temporal variations of the measured target radar cross section (RCS). For complex or stealth targets, small variations in the target range and orientation with respect to the sensor could result in large RCS variations (e.g. 20 dB), thus inevitably leading to significant degradations of the signal-to-noise ratio (SNR).

Multistatic radars, which employ multiple closely and/or widely separated transmitting and receiving radar nodes to monitor a common surveillance area [1], can capture a larger percentage of the power backscattered from the target, by virtue of different transmitter-target-receiver geometries (i.e. aspect diversity). However, due to realization costs and strong sensor deployment constraints, the radar nodes seldom cooperate with each other. In fact, they typically provide the central node, i.e. the one responsible for information fusion, with their pre-elaborated pictures of the surveyed area (i.e. decentralized processing). This local pre-processing limits the synchronization procedure only to time and reduces the amount of data to be shared between the remote nodes and the fusion center. However, the information extraction process is not truly maximized.

The multiple input multiple output (MIMO) approach for networked radars grants better coordination and information extraction than the multistatic radar approach [2]. The main difference between the two radar architectures is in the capability of MIMO radars to jointly process the data streams coming from all the remote

For further author information, send correspondence to Salvatore Maresca:
E-mail: salvatore.maresca@santannapisa.it, Telephone: +39050882233.

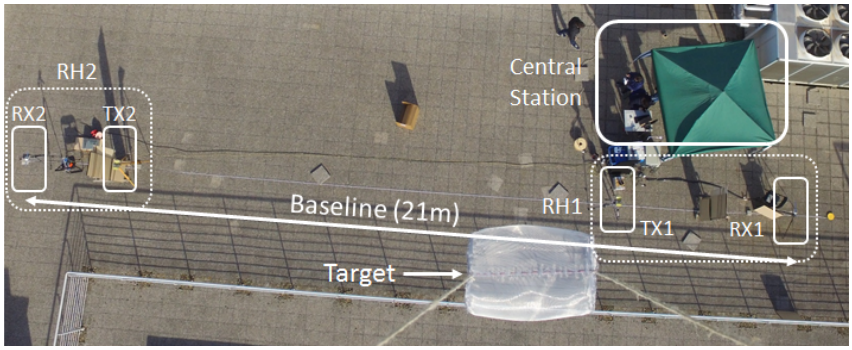

Figure 1. Aerial picture of the test field, taken by one of the drones carrying the targets. The target is the metal net cylinder hanging from the drone on a twine.

nodes, which directly transfer the raw received signals to the central node for data fusion (i.e. centralized processing). This solution, which requires high-bandwidth communication links, ideally maximizes the informative content that can be extracted from the raw data. The structural differences between multistatic and MIMO radar systems together with a comprehensive performance comparison can be found in [3].

Unfortunately, the pratical implementation of MIMO radars with widely separated antennas is hindered by two main problems. The first one is the necessity of precise time/phase synchronization among the carrier signals at the radar nodes. Since networked radars are typically operated with physically different local oscillators, each of them suffering from statistically independent phase offsets, proper solutions must be necessarily found [4]. The second problem is how to guarantee a reliable bi-directional large-bandwidth long-range signal distribution among the remote nodes and the fusion centre. Up to now, these two issues represent the main limitation factor to the development of such systems in real operative scenarios [5].

Recently, photonic technology has been investigated to implement the main functionalities of microwave systems. The goal is to overcome the actual limitations of electronic devices and subsystems and, possibly, to replace them. In this sense, photonics has demonstrated several properties that are fundamental for developing future radar systems [5–7]: low phase noise due to the excellent spectral purity of lasers, generation of ultra-wide bandwidth signals (i.e. up to tens of GHz with carriers in the mm-waves), easy tunability of lasers and optical devices (e.g. filters) enabling waveform diversity, low loss/distortion signal propagation via optical fiber links, immunity to electromagnetic interference and eavesdropping. The possibility to guarantee long-time phase stability and frequency/phase coherence between the transmitted and received signals [8], as well as the possibility to distribute the signals by means of optical fiber links, assures high-quality/coherence and the needed long-range large-bandwidth connectivity between the radar remote nodes [9]. These features make photonics very appealing for the development of future coherent radar networks with widely separated antennas [5].

In this work, the proposed radar network is based on photonics for the local oscillator generation and for the peripherals remoting, exploiting radio-over-fiber (RoF) techniques. The first coherent radar system based on photonics [10] and the results presented in [11] have fostered the development of the first photonics-based radar network demonstrators in outdoor environments [12, 13]. These experiments have been conducted within the SOLE project, with the final aim of designing and implementing the demonstrator of a fully-operational multiband centralized radar network based on photonic technology.

This paper focuses on presenting the main achievements from the radar network side and the proposed coherent data fusion strategy applied to real experimental data acquired in a controlled outdoor scenario on the rooftop of our lab, see Fig. 1. Finally, starting from the promising results presented in [12, 13], a modified version of the cell-averaging constant false alarm rate (CA-CFAR) detection algorithm is applied in which the decision threshold is evaluated from the bistatic range cells around the cell-under-test (CUT) [14]. Far from being exhaustive, this paper aims at considering and addressing some of the main architectural and signal processing issues that will rise from a real operative scenario, in which a multiband coherent MIMO radar based on photonic technology will be operated in a real maritime surveillance scenario within SOLE.

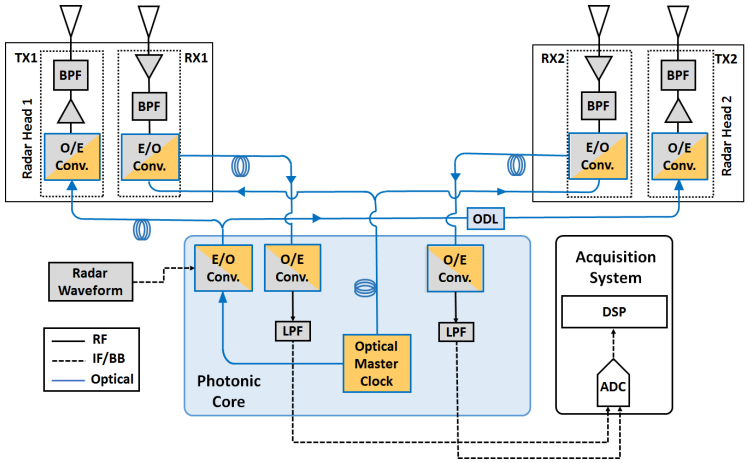

Figure 2. Architecture of the proposed Photonic Radar Network. DSP: Digital Signal Processing; ADC: Analog-to-Digital Converter; RF: Radio Frequency; LPF: Low-Pass Filter; E/O: Electro-Optical; ODL: Optical Delay Line; O/E: Opto-Electrical; IF/BB: Intermediate Frequency/Base Band; BPF: Band-Pass Filter.

2. PHOTONIC RADAR NETWORK ARCHITECTURE

For an initial validation of the proposed radar network architecture, a preliminary demonstrator has been developed. The demonstrator, depicted in Fig. 2, is based on a photonics-based radar transceiver (i.e. the photonic core) for signal generation/detection, a co-located acquisition system and two radar heads (RHs) with one transmitter (TX) and one receiver (RX) each. The RHs are remoted by means of radio-over-fiber (RoF) links.

Photonics-Based Radar Transceiver

The main building element of the photonic core is the optical master clock [10–13], which consists in a solid-state mode-locked laser (MLL), i.e. a pulsed laser whose optical spectrum is a combination of several phase-locked lines. These lines are spaced by the MLL pulse repetition frequency $f_{MLL} = 400$ MHz. The MLL allows to generate multiple radio-frequency (RF) carriers with very low phase noise, upon the opto-to-electronic (O/E) conversion of the MLL laser in a photodiode (PD) [8]. The same MLL is used for both signal up- and down-conversion, ensuring a perfect synchronization of the RHs and preserving the coherence of the signals.

In up-conversion, the radar signal, digitally generated at intermediate frequency (IF), is modulated on the MLL spectrum by an electro-to-optic (E/O) modulator. Then, it is photo-detected, generating replicas at $kf_{MLL} \pm f_{IF}$, with k positive integer and with $f_{IF} = 100$ MHz [9,10]. The desired RF output carrier frequency f_{RF} can be selected by means of a band-pass microwave filter (BPF), centered at f_{RF} and with bandwidth larger than $B = 100$ MHz. In down-conversion, the RF signal is similarly modulated on the MLL, then the O/E conversion at the PD generates again replicas of the RF signal down-converted at $kf_{MLL} \pm f_{IF}$, including $k = 0$ [9]. The large MLL optical spectrum ensures high efficiency, while the wide E/O and O/E bandwidth of the available modulators and PDs allows for the flexible management of RF signals up to several tens of GHz [8].

In [15], a coherent dual-band system operating at 2.5 GHz in (S-band) and 10 GHz (X-band), exploiting the same f_{MLL} and with 20 MHz signal bandwidth, was described and its performance evaluated. The transmitter generated signals with a time jitter of 15 fs (integrated from 100 Hz), exhibiting a spurious free dynamic range (SFDR) > 70 dB over 20 MHz, and a SNR of 73 dB/MHz. The receiver subsystem had an overall timing jitter of 10 fs in the same integration interval, enabling a SFDR of 50 dB and a noise figure (NF) of 8 dB. The minimum detectable signal was -122 and -124 dBm, in the S- and X-band respectively. In [10,11], the proposed photonic radar demonstrator was compared with an X-band commercial radar system, achieving comparable performance, with the additional feature of frequency flexibility to cope with sprectum crowding.

Radio-over-Fiber Signal Distribution

Since the RF signals are loaded on an optical carrier, the TXs/RXs at the RHs are connected with the photonic core through spans of single-mode fiber (SMF), depicted by the blue coils in Fig. 2. Thus, a RoF system is implemented [16]. Optical fibers grant small propagation losses (i.e. in the order of 0.2 dB/km), absence of electromagnetic interference, and preservation of signal coherence [9]. The optical delay line (ODL), implemented using a 1 km SMF spool inserted before the TX of RH2, generates the time diversity between RH1 and RH2.

Commercial RoF systems ensure an analog bandwidth up to 20 GHz with a gain of -25 dB (external modulation and no external RF amplification), SNR up to 146 dB/Hz, a SFDR up to 109 dBHz, and a NF of 38 dB. Otherwise, if external RF amplification is employed, a gain of 18 dB and a NF of 19 dB can be obtained, at the expenses of SNR and SFDR that slightly decrease to 140 dB/Hz and 101 dBHz, respectively. The linearity of the link can be improved by employing linearized or dual-output E/O modulation, and/or by keeping the power at suitable levels to avoid non-linear phenomena in the optical fiber. However, in RoF applications for radar systems, the intrinsic chromatic dispersion (CD) of optical fibers can represent an additional issue. This can be easily cancelled, e.g. by inserting in the link a span of CD-compensating fiber, or by employing single side-band modulation. A comprehensive analysis of the aforementioned issues and solutions can be found in [7] and references therein.

Radar Heads

Once the E/O converted radar waveform is delivered to a TX, this operates the O/E conversion, by which implies the band-pass filtering the signal at the desired RF carrier. The employed BPFs are multi-cavity filters are centered at $f_{RF} = 9.7$ GHz. Finally, after the amplification stage, the radar signal is transmitted by the antenna. The employed antennas at the TXs are ultra-wideband Vivaldi-shaped horn antennas with about 50° aperture and 12 dBi maximum gain. The RXs are equipped with very similar antennas. The detected radar echoes received by the RHs antennas are amplified, pass-bandband-pass filtered and E/O converted. Then, the received signals are transmitted back to the photonic core and O/E converted. After this operation, the signals from each RX are low-pass filtered and fed into a two-channel acquisition system, where they are digitized by an analog-to-digital converter (ADC) at 400 MS/s per channel.

3. SIGNAL PROCESSING SCHEME

The proposed radar network architecture allows to achieve excellent phase coherence, thus making the proposed radar network architecture ideal for coherent MIMO processing. First, the same optical clock (i.e. the MLL) is used in transmission for the up-conversion and in reception for the down-conversion of all the signals. Second, the employed optical oscillator is a kind of laser that is usually characterized by very low phase noise [8]. If the angular jitter of the overall architecture is lower than 10^{-1} rad, the negative effects on MIMO coherent detection due to sidelobe increase can be neglected [17]. Otherwise, phase jitter could negatively affect not only target detection performance, but also increase the sidelobe level, thus introducing additional false alarms. Finally, the temporal jitter of the considered system architecture, which corresponds to the integration of the oscillator phase noise for the offset frequencies in the interval [20 Hz, 200 MHz], is in the order of 10^{-12} s, while the angular jitter is in the order of 10^{-2} rad, lower than the limit reported in [17].

3.1 Radar Signal Model and MIMO Processing

In the general case of a radar network composed by M TXs and N RXs, the photonic core shall have N ADCs which digitize the received signals. These signals, down-converted at f_{IF}, are the linear combination of the M echo signals from each TXs. The subscript k,l indicates the generic virtual channel, determined by the k^{th} TX and l^{th} RX, for $k = 1,\ldots,M$ and $l = 1,\ldots,N$. Each of the N digitized signals is split into the M individual bistatic channels for data processing. To maximize the SNR, pulse compression is performed on the complex received base-band (BB) signals, as detailed in [11–13]. Thus, the signal $r_{k,l}(t)$ can be written as:

$$r_{k,l}(t) = a_{k,l}(x,y) \cdot s_k\left(t - \tau_{k,l}(x,y)\right) e^{j[\theta(t-\tau_{k,l}(x,y))-\theta(t)]} + n_{k,l}(t), \tag{1}$$

where $s_k(t)$ is the signal transmitted by the k^{th} TX, $a_{k,l}(x,y)$ is an amplitude factor, while $\tau_{k,l}(x,y)$ is the time delay proportional to the bistatic distance. Both are functions of the target location (x,y) and the positions of

on the k^{th} TX and l^{th} RX positions in the Cartesian plane. For simplicity, the term $n_{k,l}(t)$ is modelled as an additive white Gaussian noise (AWGN) stochastic process, while the term $\theta(t)$ takes into account the phase shift caused by the oscillator instability. Finally, the following log-likelihood function represents the "fused" coherent MIMO output:

$$ln\left[f\left(r\left(t\right)|\left(x,y\right)\right)\right] = c' \cdot \left| \sum_{k=1}^{M} \sum_{l=1}^{N} e^{-j2\pi f_{IF} \tau_{k,l}(x,y)} \cdot \int r_{k,l}^{BB*}(t) \cdot s_{k}^{BB} \ \left(t - \tau_{k,l}\left(x,y\right)\right) dt \right| + c''. \tag{2}$$

According to eq. (2), for each possible target location with coordinates (x, y), the decision statistic is computed determining, for all the M TXs and N RXs, the correlation between the received and transmitted baseband equivalent signals, denoted by $r_{k,l}^{BB}(t)$ and $s_{k}^{BB}(t)$ respectively, while $*$ is the complex conjugation operator. In addition to this, the exponential terms $e^{-j2\pi f_{IF}\tau_{k,l}(x,y)}$ re-align the phases of the signals after they have travelled different TX-target-RX paths. After this re-phasing, all the $M \times N$ correlation contributes are summed together coherently. For details about c' and c'', and a complete mathematical description, please refer to [17].

3.2 CFAR Detection applied to MIMO Radar

Target detection based on the CFAR paradigm applied to MIMO radars has been to subject of many works, some of which are reported in [18]. In [19], the optimal detector in the Neyman-Pearson sense is derived in white Gaussian noise with known variance, together with the uniformly most powerful invariant (UMPI) detector having the CFAR property in the case of unknown noise variance. The problem of detection in non-Gaussian clutter has been considered in [20–22], while multi-pulse detection schemes were presented in [23]. However, to satisfy the CFAR property, adaptive threshold techniques are necessary. Among these, the most common one is the CA-CFAR, which estimates the mean noise power from a set of reference cells. The CA-CFAR strategy is the optimal detector only when the input noise to the square law detector is Gaussian and homogeneous, while it suffers performance degradation in non-homogeneous environments [24].

Here, following the methodology described in [18], we consider a 2D detection problem in which the statistic Y is the MIMO cross-ambiguity function described by eq. (2) in the Cartesian space. The detection threshold is usually proportional to the estimate of total noise power and it is obtained by processing the contents of K reference cells surrounding the CUT, except for N_G guard cells, which are not considered in the calculation. In this way, the statistic Y is compared with a threshold such that, if $Y \geq T \cdot Z$, we decide for the "target present" hypothesis (i.e. H_1); we decide for the "target absent" (i.e. H_0) otherwise.

The detection threshold is the product of two factors: T is the scale factor that depends on the desired constant false alarm probability, (i.e. P_{FA}), while Z is the noise power estimate. This procedure is repeated for all the (x, y) coordinates into which the Cartesian plane is discretized. As mentioned, instead of the classic rectangular window centered around the CUT, we consider the union of the isorange ellipsoids of each TX-RX radar node. This choice is motivated by the possible presence in the final MIMO cross-ambiguity function of sidelobes distributed along the isorange ellipsoids. Especially when M and N are small, these ellipsoids may lead to very high sidelobes and, thus, cause a significant increase of false alarms [14].

4. EXPERIMENTAL RESULTS

In our experiment, we further investigate the network presented in [14] and we test it in a real outdoor scenario, on the rooftop of our lab, with multiple closely-spaced targets, see Fig. 1. The network is composed of two TXs and two RXs, connected with the photonic core through optical fiber links. At the actual status of development, the photonic core generates a 100 MHz-bandwidth linear frequency modulated upsweep chirp signal with 100 ns duration, pulse repetition interval (PRI) of 50 μs and $B = 100$ MHz centered at $f_{RF} = 9.7$ GHz, corresponding to a range resolution of 1.5 m. The two transmitted waveforms are separated in the time domain with an ODL on the path between the photonic core and RH2. The network is deployed, according to the scheme in Fig. 3, with the four antennas aligned over a 21 m baseline. These are oriented upwards, to mitigate clutter and multipath returns due to the surrounding structures, buildings and vegetation, and to ensure the simultaneous illumination of both targets. The output power from the TX antennas is ≈ 100 mW.

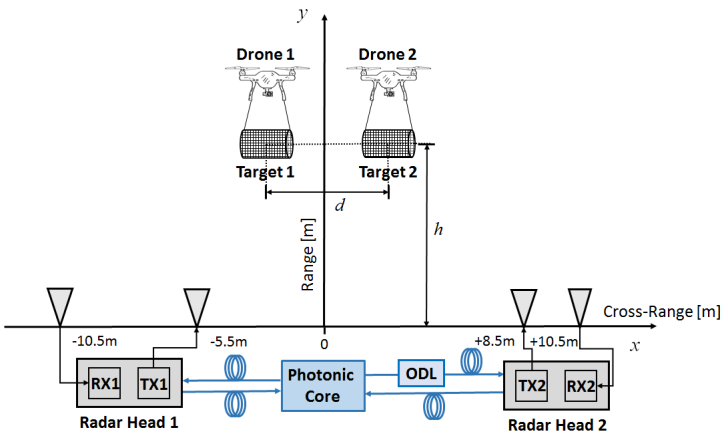

Figure 3. Geometry of the coherent photonics-based MIMO radar network and in-field experimental setup.

The targets consist of two cylinders, with 17 cm radius and 50 cm height, made of a tight-mesh metal net and hanging from two commercial mini-drones (Fig. 1). The height h of the two targets was controlled and kept always between 15 and 20 m, while the two drones were always kept hovering at the same height with respect to each other and separated by a cross-range distance $d = 3$ m to avoid possible collisions. Unfortunately, it was not possible to univocally determine the exact position of the drones.

Let us consider a 2D detection problem, in which the output of eq. (2) undergoes CA-CFAR detection in the search space. The reference cell parameters are $K = 20$ and $N_G = 20$, for both the rectangular window and the proposed methods, respectively in Fig. 4(a) and Fig. 4(b). As it will be discussed in the following, by using the proposed range-gating method, the effect of the constant bistatic-range ellipsoids intersecting at target pixels results strongly mitigated. Thus, we expect a reduction of the number of false alarms originated by the target.

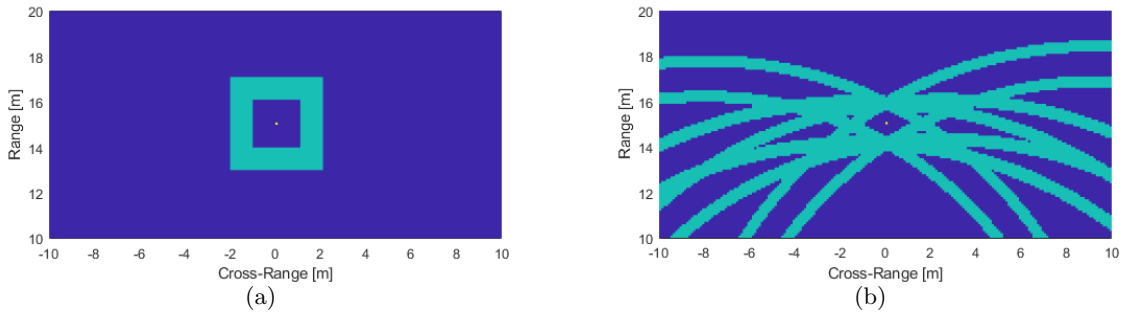

Figure 4. Reference cells (green) for the CUT (yellow) at $(0, 15)$ m in the Cartesian plane: (a) the classic rectangular window, (b) the proposed method based on the combination of bistatic ellipsoids. Detector parameters: $K = 20$, $N_G = 20$.

A 25 ms integration time (i.e. 500 PRIs) has been considered for the coherent MIMO processing output, which is evaluated in a search space of 151×301 samples in the interval $[5, 20]$ m and $[-15, +15]$ m (i.e. 10 cm spacing), along range and cross-range respectively. Results of the coherent MIMO processing and the CA-CFAR detection strategy are depicted in Fig. 5(a) and 5(b), respectively. As we can observe in Fig. 5(a), the two targets can be separated in cross-range only by processing coherently the data. The presence of high sidelobes in the monitored area is due not only to the presence of clutter and multipath, but also to the reduced MIMO configuration (i.e. few TXs and RXs). In this sense, a larger number of TXs and RXs would significantly reduce the intensity of the peaks and grant a finer cross-range resolution. The presence of a long spool of fiber (i.e. the ODL) simulates

a distance of about 1 km between the two RHs. However, the results demonstrate the low attenuation and negligible phase distortion introduced by the fiber. The employed network is characterized by widely distributed antennas, since the four channels are spatially decorrelated, according to the definition proposed in [2]. Thus, as we can observe, aspect diversity is a key parameter to cope with target RCS fluctuations; it represents the main difference between MIMO radars and phased arrays having the same number of elements [2].

Fig. 5(b) depicts the output of the modified CA-CFAR detection algorithm. With respect to the nominal aperture of the antenna (e.g. given the distance from the baseline of 18 m and the 50° antenna aperture, the expected monostatic cross-range resolution should be about 15.7 m), the cross-range resolution has been improved by a factor of about 5. Unfortunately, due to the low emitted power and the small drone RCS, it is almost impossible to detect the two drones without applying also Doppler processing. In conclusion, given the reduced radar array configuration and the non-idealities introduced by the environment and target RCS fluctuations, the results achieved in terms of cross-range resolution can be truly considered a remarkable achievement, aimed to design and implement future coherent MIMO radars with widely separated antennas based on photonic technology.

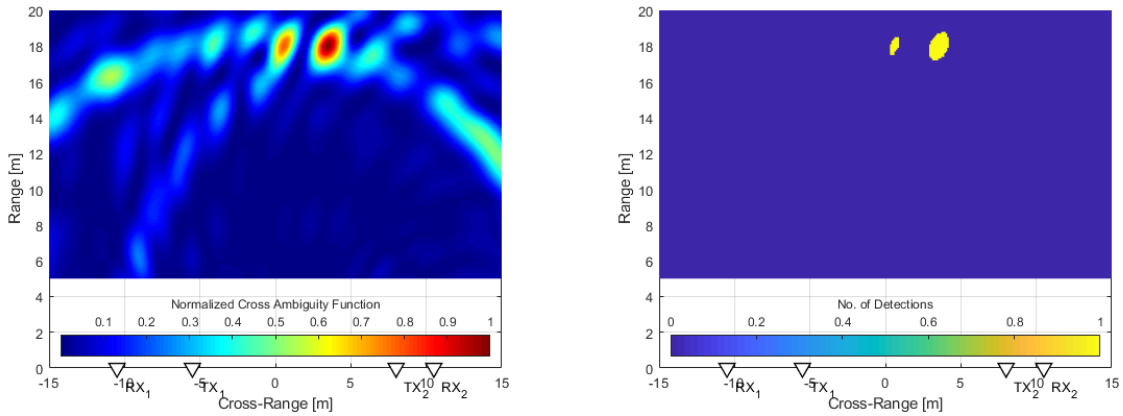

Figure 5. (a) Coherent MIMO output and (b) CA-CFAR detection output, based on the combination of bistatic ellipsoids. Detector parameters: $K = 20$, $N_G = 20$, $P_{FA} = 10^{-4}$.

5. CONCLUSIONS

In this paper, a coherent MIMO radar network demonstrator based on photonic technology has been presented and tested in a real outdoor environment within the NATO-funded SOLE Project. Two cooperative closely-spaced targets have been considered during the trials to prove the validity of the proposed architecture. They have been successfully resolved in cross-range by applying coherent MIMO processing and correctly detected by means of a modified version of the CA-CFAR detection strategy. With respect to the nominal aperture of the antenna, the cross-range resolution has been improved by a factor of five.

The contribution of photonics in preserving signal coherence among the TX and RX elements and in granting large-bandwidth long-range undistorted signal distribution over fiber is apparent. The robust features in terms of time/phase coherency allow to fully advantage from coherent MIMO processing in combination with the system geometry. These confirm that photonics is an enabling technology for coherent MIMO radars with widely distributed antennas. However, the results presented in this paper must be considered just as a first milestone, aimed to guide us through the development of a more complex radar network, with a significantly larger number of TX and RX antennas, and specifically tailored to real-time surveillance tracking and imaging applications.

ACKNOWLEDGMENTS

This work has been partially supported by the NATO SPS SOLE project.

REFERENCES

[1] Chernyak, V. S., [*Fundamentals of Multisite Radar System*], Gordon & Breach Science Publ., London (1998).

[2] Haimovich, A. M., Blum, R. S., and Cimini, L. J., "MIMO radar with widely separated antennas," *IEEE Signal Processing Magazine* **25**(1), 116–129 (2008).

[3] Gorji, A. A., *Localization, tracking, and antenna allocation in multiple-input multiple-output (MIMO) radars*, PhD thesis, McMaster University, Hamilton, Ontario (2012).

[4] Yang, Y. and Blum, R. S., "Phase synchronization for coherent MIMO radar: Algorithms and their analysis," *IEEE Transactions on Signal Processing* **59**, 5538–5557 (Nov. 2011).

[5] Bogoni, A., Ghelfi, P., and Laghezza, F., [*Photonics for Radar Networks and Electronic Warfare Systems*], IET SciTech Publishing, London (2019).

[6] Lembo, L., Ghelfi, P., and Bogoni, A., "Analysis of a coherent distributed MIMO photonics-based radar network," in [*European Radar Conference*], 170–173 (Sep. 2018).

[7] Serafino, G., Scotti, F., Lembo, L., Hussain, B., Porzi, C., Malacarne, A., Maresca, S., Onori, D., Ghelfi, P., and Bogoni, A., "Toward a new generation of radar systems based on microwave photonic technologies," *Journal of Lightwave Technology* **37**, 643–650 (Jan 2019).

[8] Serafino, G., Ghelfi, P., Perez-Millan, P., Villanueva, G. E., Palaci, J., Cruz, J. L., and Bogoni, A., "Phase and amplitude stability of EHF-band radar carriers generated from an active mode-locked laser," *Journal of Lightwave Technology* **29**, 3551–3559 (Dec. 2011).

[9] Williams, P. A., Swann, W. C., and Newbury, N. R., "High-stability transfer of an optical frequency over long fiber-optic links," *J. Opt. Soc. Am. B* **25**, 1284–1293 (Aug. 2008).

[10] Ghelfi, P., Laghezza, F., Scotti, F., Serafino, G., Capria, A., Pinna, S., Onori, D., Porzi, C., Scaffardi, M., Vercesi, V., Lazzeri, E., Berizzi, F., and Bogoni, A., "A fully photonics-based coherent radar system," *Nature* **507**, 341–345 (Mar. 2014).

[11] Laghezza, F., Scotti, F., Serafino, G., Banchi, L., Malaspina, V., Ghelfi, P., and Bogoni, A., "Field evaluation of a photonics-based radar system in a maritime environment compared to a reference commercial sensor," *IET Radar, Sonar Navigation* **9**(8), 1040–1046 (2015).

[12] Lembo, L., Maresca, S., Serafino, G., Scotti, F., Amato, F., Ghelfi, P., and Bogoni, A., "In-field demonstration of a photonic coherent MIMO distributed radar network," in [*IEEE Radar Conf.*], (Apr. 2019).

[13] Maresca, S., Serafino, G., Scotti, F., Amato, F., Lembo, L., Bogoni, A., and Ghelfi, P., "Photonics for coherent MIMO radar: an experimental multi-target surveillance scenario," in [*Int. Radar Symp.*], (2019).

[14] Maresca, S., Bogoni, A., and Ghelfi, P., "CFAR detection applied to MIMO radar in a simulated maritime surveillance scenario," in [*European Radar Conference*], (Oct. 2019).

[15] Ghelfi, P., Laghezza, F., Scotti, F., Onori, D., and Bogoni, A., "Photonics for radars operating on multiple coherent bands," *Journal of Lightwave Technology* **34**, 500–507 (Jan 2016).

[16] Beas, J., Castanon, G., Aldaya, I., Aragon-Zavala, A., and Campuzano, G., "Millimeter-wave frequency radio over fiber systems: A survey," *IEEE Communications Surveys Tutorials* **15**(4), 1593–1619 (2013).

[17] Lehmann, N. H., Haimovich, A. M., Blum, R. S., and Cimini, L., "High resolution capabilities of MIMO radar," in [*2006 Fortieth Asilomar Conference on Signals, Systems and Computers*], 25–30 (Oct. 2006).

[18] Janatian, N., Modarres-Hashemi, M., and Sheikhi, A., "CFAR detectors for MIMO radars," *Circuits, Systems, and Signal Processing* **32**, 1389–1418 (Jun. 2013).

[19] Fishler, E., Haimovich, A., Blum, R. S., Cimini, L. J., Chizhik, D., and Valenzuela, R. A., "Spatial diversity in radars—models and detection performance," *IEEE Trans. on Sig. Proc.* **54**, 823–838 (March 2006).

[20] Cui, G., Kong, L., Yang, X., and Yang, J., "The rao and wald tests designed for distributed targets with polarization mimo radar in compound-gaussian clutter," *Circ., Sys., and Sig. Proc.* **31**, 237–254 (Feb 2012).

[21] Chong, C. Y., Pascal, F., Ovarlez, J., and Lesturgie, M., "Mimo radar detection in non-gaussian and heterogeneous clutter," *IEEE Journal of Selected Topics in Signal Processing* **4**, 115–126 (Feb 2010).

[22] Xun Chen and Blum, R., "Non-coherent mimo radar in a non-gaussian noise-plus-clutter environment," in [*2010 44th Annual Conference on Information Sciences and Systems (CISS)*], 1–6 (March 2010).

[23] Sheikhi, A. and Zamani, A., "Temporal coherent adaptive target detection for multi-input multi-output radars in clutter," *IET Radar, Sonar Navigation* **2**, 86–96 (April 2008).

[24] Gandhi, P. P. and Kassam, S. A., "Analysis of CFAR processors in nonhomogeneous background," *IEEE Transactions on Aerospace and Electronic Systems* **24**, 427–445 (Jul. 1988).